Article

Cell Reports

GRK2 Fine-Tunes Circadian Clock Speed and Entrainment via Transcriptional and Post-translational Control of PERIOD Proteins

Graphical Abstract

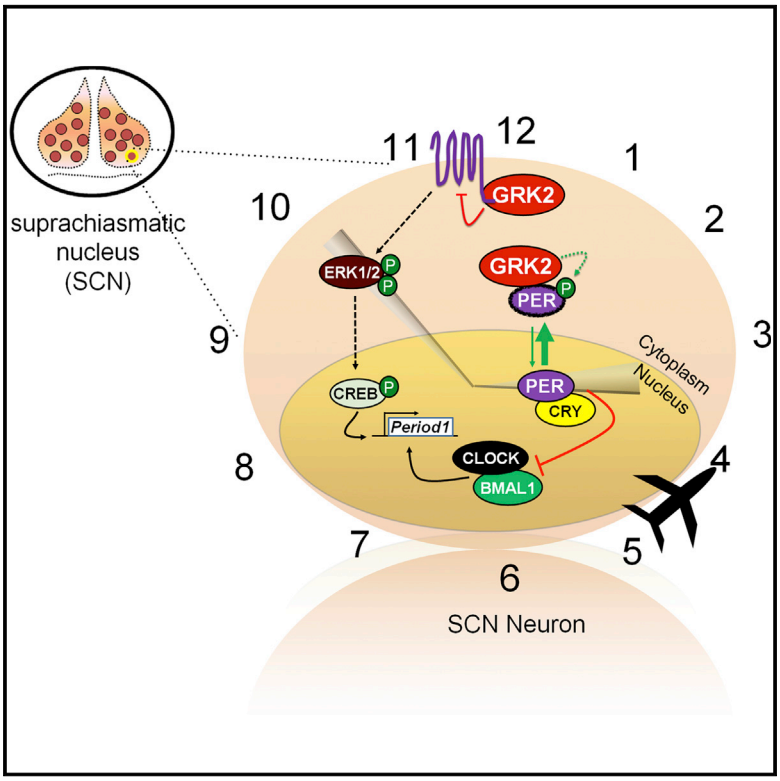

Highlights

- GRK2 ablation alters light-induced entrainment and delays recovery from jetlag
- GRK2 ablation increases circadian amplitude and decreases circadian period
- GRK2 suppresses *mPeriod1* transcription and PERIOD1/2 nuclear trafficking
- GRK2 physically binds to PERIOD1/2 and promotes PERIOD2 phosphorylation

Authors

Neel Mehta, Arthur H. Cheng, Cheng-Kang Chiang, ..., Bo Xu, Daniel Figeys, Hai-Ying M. Cheng

Correspondence

haiying.cheng@utoronto.ca

In Brief

Mehta et al. demonstrate the importance of GRK2 in regulating both the pace of the circadian clock and its response to environmental time cues (i.e., light). GRK2 functionally interacts with the molecular clock at the transcriptional and post-translational levels, dampening *mPeriod1* gene transcription and suppressing nuclear trafficking of PERIOD1/2 proteins.

Mehta et al., 2015, Cell Reports *12*, 1272–1288
August 25, 2015 ©2015 The Authors
http://dx.doi.org/10.1016/j.celrep.2015.07.037

OPEN ACCESS
CellPress

Cell Reports
Article

GRK2 Fine-Tunes Circadian Clock Speed and Entrainment via Transcriptional and Post-translational Control of PERIOD Proteins

Neel Mehta,[1,2,4] Arthur H. Cheng,[1,2,4] Cheng-Kang Chiang,[3,4] Lucia Mendoza-Viveros,[1,2,4] Harrod H. Ling,[1,2] Abhilasha Patel,[1] Bo Xu,[3] Daniel Figeys,[3] and Hai-Ying M. Cheng[1,2,*]

[1]Department of Biology, University of Toronto Mississauga, 3359 Mississauga Road, Mississauga, ON L5L 1C6, Canada
[2]Department of Cell and Systems Biology, University of Toronto, 25 Harbord Street, Toronto, ON M5S 3G5, Canada
[3]Ottawa Institute of Systems Biology, Department of Biochemistry, Microbiology and Immunology and Department of Chemistry and Biomolecular Sciences, University of Ottawa, 451 Smyth Road, Ottawa, ON K1H 8M5, Canada
[4]Co-first author
*Correspondence: haiying.cheng@utoronto.ca
http://dx.doi.org/10.1016/j.celrep.2015.07.037

SUMMARY

The pacemaker properties of the suprachiasmatic nucleus (SCN) circadian clock are shaped by mechanisms that influence the expression and behavior of clock proteins. Here, we reveal that G-protein-coupled receptor kinase 2 (GRK2) modulates the period, amplitude, and entrainment characteristics of the SCN. *Grk2*-deficient mice show phase-dependent alterations in light-induced entrainment, slower recovery from jetlag, and longer behavioral rhythms. *Grk2* ablation perturbs intrinsic rhythmic properties of the SCN, increasing amplitude and decreasing period. At the cellular level, GRK2 suppresses the transcription of the *mPeriod1* gene and the trafficking of PERIOD1 and PERIOD2 proteins to the nucleus. Moreover, GRK2 can physically interact with PERIOD1/2 and promote PERIOD2 phosphorylation at Ser545, effects that may underlie its ability to regulate PERIOD1/2 trafficking. Together, our findings identify GRK2 as an important modulator of circadian clock speed, amplitude, and entrainment by controlling PERIOD at the transcriptional and post-translational levels.

INTRODUCTION

Circadian timekeeping mechanisms evolved to allow organisms to anticipate and respond to cyclical changes in their environment (Reppert and Weaver, 2002). In mammals, the central circadian pacemaker, the suprachiasmatic nucleus (SCN), dictates the tempo of physiological and behavioral rhythms to near-24-hr periodicity through generation and maintenance of self-sustained rhythms, which in turn are synchronized to environmental day-night cycles by the process of photic entrainment (Moore, 2013). The molecular basis of circadian rhythms involves a set of core clock proteins that interact in a series of transcription-translation feedback loops (TTFLs) to drive their own rhythmic gene expression (Reppert and Weaver, 2002). Heterodimers of CLOCK-BMAL1 transcription factors activate E-box-mediated transcription of *Period* (*Per*) and *Cryptochrome* (*Cry*) genes. The subsequent translocation of PER and CRY proteins to the nucleus closes the feedback loop by repressing CLOCK-BMAL1-dependent transcription. Photic entrainment also relies on transcriptional activation of *period* genes within the SCN (Akiyama et al., 1999). However, beyond transcription, mechanisms that control protein translation or post-translational modifications (e.g., phosphorylation) can likewise have profound effects on core clock oscillations and entrainment (Gallego and Virshup, 2007). Numerous studies have shown the importance of specific protein kinases in the transcriptional, translational, and post-translational control of the circadian clock (Gallego and Virshup, 2007).

In our search to identify key players in SCN clock regulation, we focused on G-protein-coupled receptor (GPCR) kinase 2 (GRK2). GRK2 belongs to a family of serine/threonine protein kinases that directly phosphorylate agonist-bound GPCRs and downregulate receptor-mediated signaling via receptor desensitization and/or internalization (Gurevich et al., 2012). There are seven mammalian GRKs: GRK1 through GRK7. Expression of GRK1 and GRK7 is restricted primarily to rod and cone photoreceptors, whereas the remaining GRKs are expressed in the rodent brain and in other tissues (Gurevich et al., 2012). In smooth muscle, GRK2 has been shown to mediate the desensitization of VPAC2 (Murthy et al., 2008), the receptor for vasoactive intestinal peptide (VIP), a critical neuropeptide for SCN clock function (Aton et al., 2005). *Drosophila* GRK2 has been shown to underlie circadian rhythms in olfactory responses through GPCR regulation in olfactory sensory neurons (Tanoue et al., 2008). In addition to its classical function as a GPCR kinase, GRK2 can phosphorylate non-GPCR substrates including various receptor tyrosine kinases, structural proteins (e.g., tubulin), and intracellular signaling proteins (Penela et al., 2010). GRK2 can also regulate the function of receptors and other proteins in a kinase-independent manner through direct physical association (Penela et al., 2010). The combination of its classical and

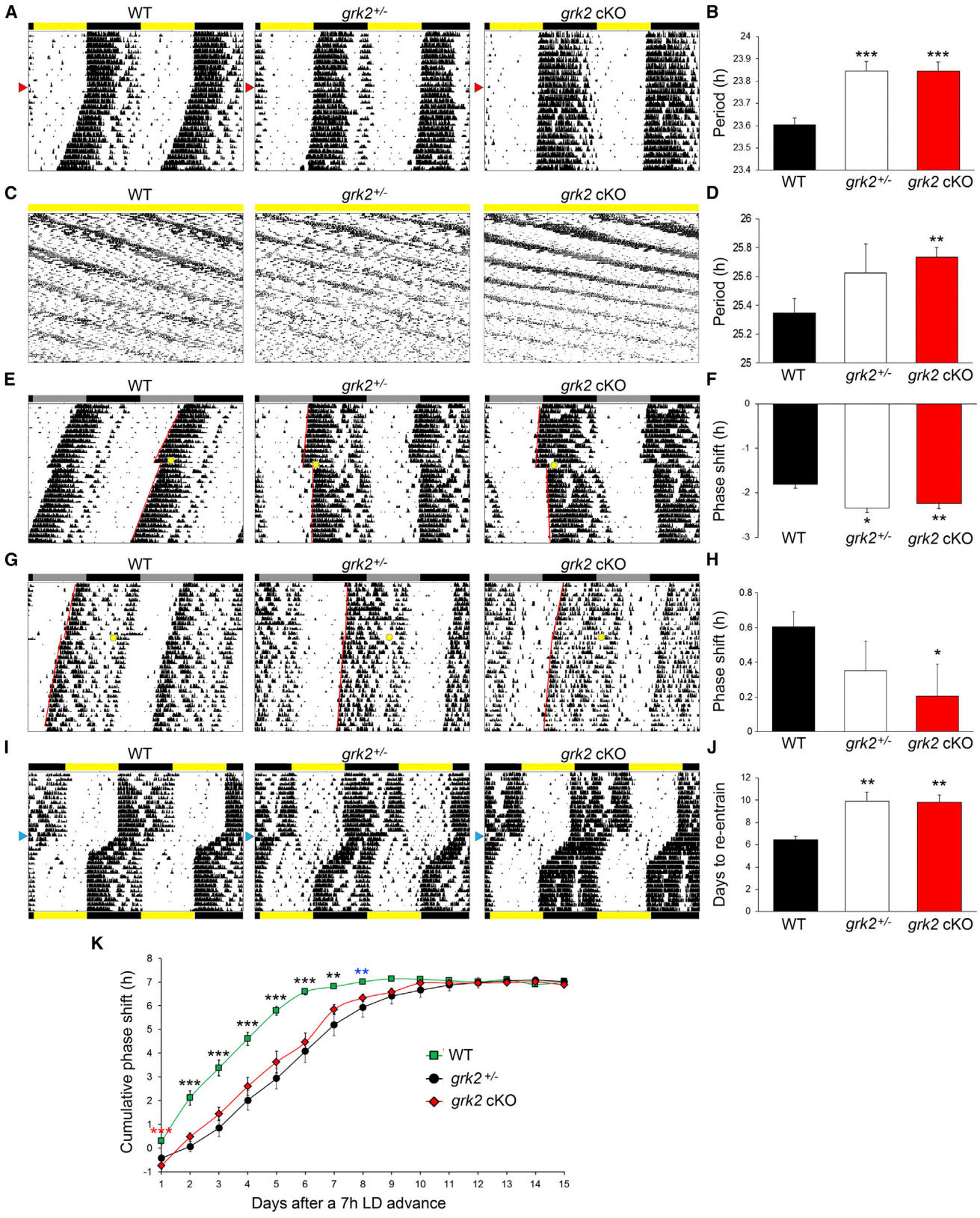

(legend on next page)

noncanonical functions prompted us to explore GRK2′s potential contribution to the regulation of the murine SCN clock. Here, we report that GRK2 is a modulator of circadian period, amplitude, and entrainment, through its effects on *mPer1* transcription and nuclear trafficking of PER1 and PER2.

RESULTS

Genetic Disruption of GRK2 in Mice Lengthens the Free-Running Behavioral Period and Alters Light-Induced Entrainment

To begin our study, we examined the temporal expression of GRK2 and other GRK family members within the murine SCN. GRK2 protein was found to be both abundant and expressed at constant levels throughout the circadian cycle (Figures S1A and S1B). qPCR analyses revealed a lack of circadian fluctuation of *grk2* at the mRNA level and the expression of *grk3*, *grk4*, and *grk5* within the SCN (Figure S1C). Of the four, only *grk3* and *grk4* exhibited rhythmic expression at the mRNA level, both peaking in the mid subjective night (Figure S1C). These results, however, do not rule out the possibility that GRK2 activity/function fluctuates in the SCN across the circadian cycle or in response to light, as exemplified by extracellular signal-regulated kinases (ERKs) 1/2 (Obrietan et al., 1998).

To investigate the function of GRK2 in the central clock, we employed two independent gene-targeted mouse models. The first is a heterozygous *grk2* (*grk2*$^{+/-}$) mouse strain generated by conventional gene targeting (Jaber et al., 1996). The second is a conditional ablation of the *grk2* gene in GABAergic neurons using a *Vgat*-IRES-Cre mouse strain (Vong et al., 2011) to drive Cre-mediated excision of the *grk2* floxed alleles (*grk2*$^{fl/fl}$; Matkovich et al., 2006) in vesicular GABA transporter (VGAT)-expressing cells. Previous studies have shown that the majority of SCN neurons are GABAergic (Moore, 2013). As expected, GRK2 protein levels in the SCN were reduced by >50% in *grk2*$^{+/-}$ mice and were negligible in *Vgat*-driven *grk2* conditional knockouts (*grk2* cKO) (Figure S1D).

Next, we assessed the circadian behavior of *grk2*$^{+/-}$ and *grk2* cKO mice using a spectrum of experimental lighting paradigms. The phase angle (ψ) of entrainment under a fixed 12-hr light:12-hr dark (LD) cycle was significantly delayed in *grk2*$^{+/-}$ and *grk2* cKO mice relative to *grk2* wild-type (WT) control mice (phase angle [h]: WT, 0.03 ± 0.03 [n = 20]; *grk2*$^{+/-}$, 0.17 ± 0.04 [n = 14]; *grk2* cKO, 0.20 ± 0.05 [n = 11]; $p < 0.05$ WT versus *grk2*$^{+/-}$; $p < 0.01$ WT versus *grk2* cKO). Consistent with the known dependence of ψ on intrinsic circadian period, both mutant strains exhibited a significantly longer free-running period under constant darkness (DD) (Figures 1A and 1B). The circadian period under long-term constant dim (10 lux) light (LL) was significantly longer in *grk2* cKO mice compared with both WT and *grk2*$^{+/-}$ mice (Figures 1C and 1D). All animals remained rhythmic under dim LL for the duration of the experiment. In terms of the acute effects of light, a brief light pulse (15 min, 30 lux) in the early subjective night (CT 15) produced larger phase delays in *grk2*$^{+/-}$ and *grk2* cKO mice compared to WT controls (Figures 1E and 1F). Light-induced phase advances (15 min, 40 lux) in the late night (CT 22) were significantly attenuated in *grk2* cKO, but not *grk2*$^{+/-}$, mice relative to WT controls (Figures 1G and 1H). There was no correlation between the period under DD and the magnitude of phase delays (Figure S1E) or phase advances (Figure S1F), suggesting that the longer period of *grk2* mutant mice does not contribute to their phase-shift phenotypes. In an experimental jetlag paradigm, mice experienced an abrupt advance of the LD cycle by 7 hr. *Grk2*$^{+/-}$ and *grk2* cKO mice took significantly longer to re-entrain to the new LD cycle relative to WT controls (Figures 1I–1K). *Grk2* ablation does not alter the expression of *grk3*, *grk4*, or *grk5* in the SCN (Figure S1G), ruling out the possibility that the observed phenotypes are due to compensatory changes in these other GRKs.

Collectively, our results show that loss of one or both copies of *grk2* slows behavioral rhythms under DD, augments light-induced phase delays, and decelerates the rate of re-entrainment to an advanced LD cycle. Deletion of both copies in GABAergic neurons is required to significantly attenuate acute photic phase advances and enhance period lengthening under dim LL.

The Effects of GRK2 on the Molecular Clock in the SCN

The longer behavioral period under DD suggests that GRK2 may influence the oscillatory properties of the core molecular clock within the SCN. In the SCN of WT mice, PERIOD1 (PER1) and PERIOD2 (PER2) protein abundance exhibited robust rhythms that peaked in the early and mid-subjective night, respectively (Figures 2A, 2B, 2F, 2G, and S2A–S2D). The amplitudes of PER1 and PER2 oscillations were significantly augmented in *grk2* cKO mice (Figures 2A, 2B, 2F, and 2G) and *grk2*$^{+/-}$ mice (Figures S2A–S2D) relative to WT control, due to increased peak expression at the expected CT. Single-cell analysis of PER immunoreactivity revealed that a greater number of SCN cells expressed high nuclear levels of PER1 and PER2 at CT14 and CT18, respectively, in the *grk2* cKO mice (Figures 2C and 2H) than in WT controls. Enhanced expression is visually

Figure 1. Loss of GRK2 Lengthens Locomotor Activity Rhythms and Alters Entrainment to Light

(A, C, E, G, and I) Representative actograms of wheel-running activities of WT, *grk2*$^{+/-}$, and *grk2* cKO mice under different light conditions. In (A), LD-entrained mice were released into DD (at red arrowhead). In (C), LD-entrained mice were released into dim LL (10 lux) for 16 weeks. In (E and G), mice in DD received a 15-min light pulse (LP; yellow dot) at (E) CT 15 or (G) CT 22. Regression lines (red) through daily activity onsets before and after the LP were used to measure phase shifts. In (I), mice were entrained to a fixed LD cycle prior to an abrupt advance of the LD cycle by 7 hr (at blue arrowhead). Horizontal colored bars above and below each actogram indicate the original and 7-hr-advanced LD cycles, respectively.

(B and D) Period under (B) DD and (D) LL conditions.

(F and H) Phase shifts to a (F) CT 15 and (H) CT 22 LP.

(J) Days to re-entrain to a 7-hr advanced LD cycle.

(K) Daily phase shifts to a 7-hr advanced LD cycle.

All values represent mean ± SEM; n = 8 to 21 mice per genotype. *$p < 0.05$, **$p < 0.01$, ***$p < 0.001$ versus WT (for B, D, F, H, and J). **$p < 0.01$, ***$p < 0.001$ versus *grk2*$^{+/-}$ and *grk2* cKO; ***$p < 0.001$ versus *grk2* cKO; **$p < 0.01$ versus *grk2*$^{+/-}$ (for K). See also Figure S1.

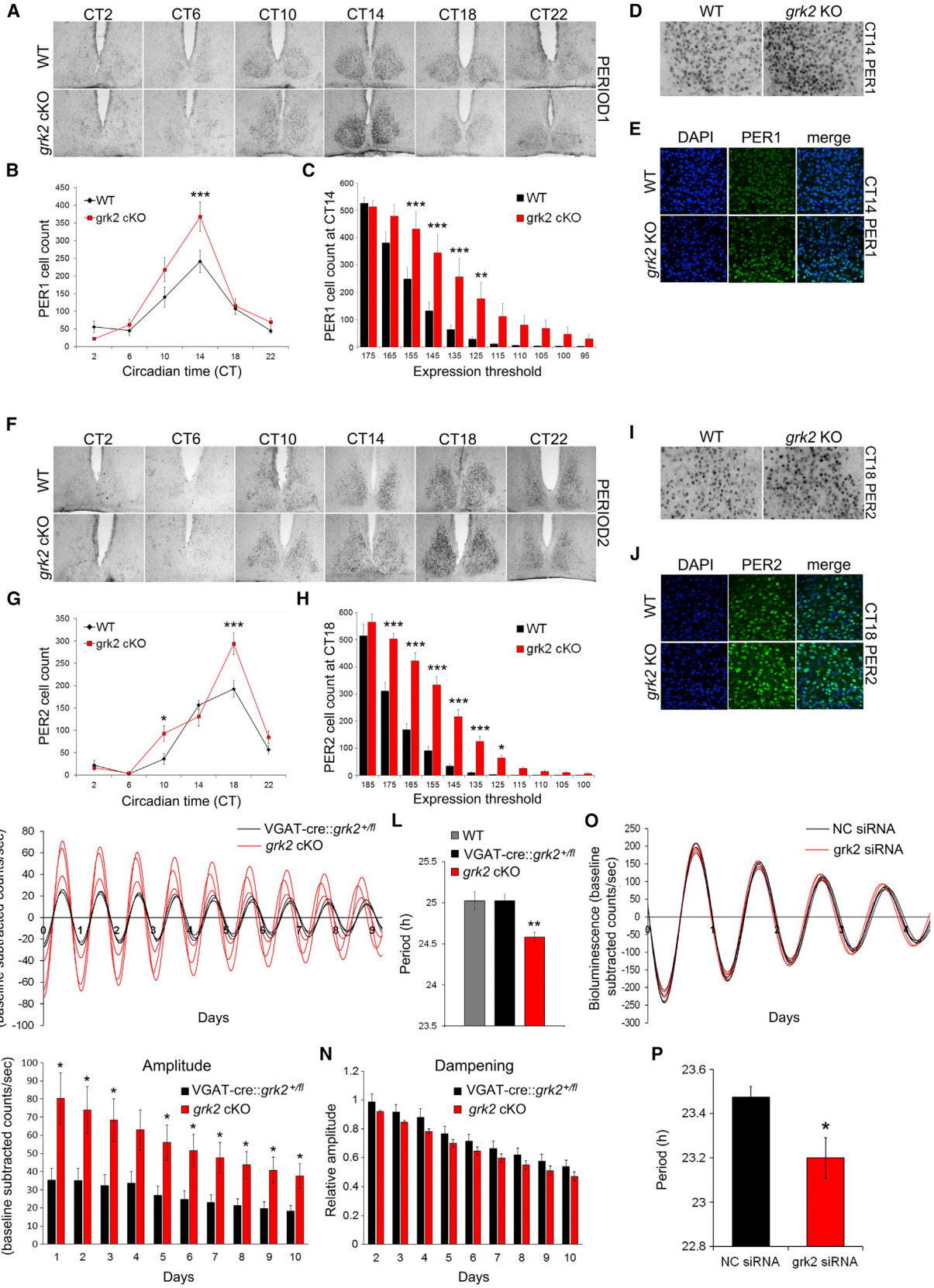

(legend on next page)

apparent in high-magnification images of the SCN immunostained for PER1 (Figures 2D and 2E) and PER2 (Figures 2I and 2J). These effects were specific to PER1/2, as we observed no change in BMAL1 protein expression in the SCN of *grk2* cKO mice across a 24-hr circadian cycle (Figures S2E and S2F).

To determine whether the circadian amplitude phenotype is intrinsic to the SCN of *grk2* cKO mice, we examined PER2::LUC bioluminescence rhythms in SCN tissue explants harvested from WT (*grk2*$^{+/+}$), VGAT-cre::*grk2*$^{+/fl}$ (heterozygous for *grk2* in GABAergic neurons), and *grk2* cKO (VGAT-cre::*grk2*$^{fl/fl}$) mice (Figure 2K). The amplitude was significantly greater in *grk2* cKO SCN compared with the two control groups (Figures 2K, 2M, and S2H). Surprisingly, the period of PER2::LUC oscillations was shortened in *grk2* cKO SCN relative to WT and VGAT-cre::*grk2*$^{+/fl}$ controls (Figures 2L and S2G). The rhythms dampened at a comparable rate across all experimental groups (Figures 2N and S2I). The shortened period of molecular rhythms was also observed in PER2::LUC murine embryonic fibroblasts (MEFs) upon small interfering RNA (siRNA)-mediated silencing of *grk2* (Figures 2O, 2P, and S2J). Collectively, our data show that GRK2 suppresses the amplitude and lengthens the period of molecular rhythms within the SCN.

The Effects of GRK2 on GPCR Internalization and Expression in the SCN

To elucidate the potential mechanisms by which GRK2 regulates the SCN clock, we first addressed the canonical function of GRK2 in GPCR desensitization and internalization. To this end, the trafficking of green/yellow fluorescent protein (GFP/YFP)-tagged versions of VIP, AVP, and PACAP receptors (VPAC2, V1b, and PAC1, respectively) were examined in Neuro2A or HEK293 cells that co-expressed either WT GRK2 or a dominant-negative kinase-deficient GRK2 (GRK2 K220R) (Kong et al., 1994). Levels of ectopic GRK2 and GRK2 K220R were similar in both cell lines (Figure S3A). Under basal (no ligand) conditions, VPAC2 receptors were localized to the plasma membrane and diffusely throughout the cytoplasm (Figure 3A), whereas V1b and PAC1 receptors were found predominantly at the plasma membrane (Figures 3C and 3D). In pcDNA3.1-transfected control cells, stimulation with VIP or AVP triggered robust internalization of VPAC2 (Figure 3A) and V1b (Figure 3C) receptors, respectively, as indicated by a strong decrease in plasma membrane fluorescence and concurrent increase in punctate cytoplasmic foci. GRK2 overexpression had no appreciable effect on the basal distribution or ligand-triggered internalization of VPAC2 and V1b receptors (Figures 3A and 3C), suggesting that the activity of endogenous GRK2 (and potentially other GRKs) is sufficient to mediate receptor trafficking. In contrast, overexpression of GRK2 K220R, which competes with endogenous GRK2 for the receptors and prevents their phosphorylation, strongly attenuated VIP-induced VPAC2 internalization without altering basal distribution (Figure 3A). The internalization of AVP-stimulated V1b receptors was less sensitive to the ameliorating effects of GRK2 K220R (Figure 3C). PAC1 receptors exhibited partial internalization in response to PACAP stimulation, as evident by the increase in cytoplasmic foci (Figure 3D). GRK2 K220R suppressed ligand-induced PAC1 internalization, whereas overexpression of GRK2 had no effect (Figure 3D). Importantly, siRNA-mediated knockdown of endogenous GRK2 (Figure S3B) had no effect on basal distribution of VPAC2 receptors but attenuated VIP-induced receptor internalization (Figure 3B), thus supporting a bona fide role of GRK2 in VPAC2 trafficking. It should be noted that up to 1 hr post-VIP stimulation, total VPAC2 levels were unaltered between *grk2* siRNA-transfected and negative control (NC) siRNA-transfected cultures and between basal and post-stimulation time points (Figure S3C).

Next, we examined the effects of *grk2* ablation on the VIP-VPAC2 system in the SCN. Time-of-day fluctuations in VPAC2 protein abundance in the SCN were markedly altered in *grk2* cKO mice (Figures 3E and 3F). Specifically, VPAC2 levels were augmented in *grk2* cKO SCN relative to WT at most time points, reaching significance at CT 14 and CT 18 (Figures 3E and 3F). *Vpac2* transcript levels in the SCN were comparable between WT and *grk2* cKO mice, suggesting a post-transcriptional effect of GRK2 on VPAC2 expression (Figure S3D). Despite the lack of change in total VPAC2 levels in our cell culture model up to 1h post-VIP stimulation, the temporal profile of VIP-VPAC2 signaling in the SCN in vivo is likely to be quite different. Given that prolonged exposure to VIP is required to induce GRK2-dependent VPAC2 degradation (Murthy et al., 2008), the most parsimonious explanation for altered VPAC2 abundance in the *grk2* cKO SCN is a reduction in internalization-coupled receptor degradation. The observed suppression in VIP levels in

Figure 2. Loss of GRK2 Increases the Amplitude of PER1 and PER2 Protein Rhythms in the SCN and Shortens Ex Vivo SCN Rhythms

(A, D–F, I, and J) Representative micrographs of (A) PER1 and (F) PER2 immunoreactivity (IR) in the SCN of WT and *grk2* cKO mice. High-magnification images of (D and E) PER1 at CT 14 and (I and J) PER2 at CT 18 by (D and I) immunohistochemistry (IHC) and (E and J) indirect IF. DAPI (blue, E and J) was used as a nuclear stain.

(B and G) Number of (B) PER1- and (G) PER2-IR nuclei in the SCN as a function of CT. Threshold was set at 150 and 160 for PER1 and PER2, respectively.

(C and H) Intensity distribution of (C) PER1 at CT 14 and (H) PER2 at CT 18 based on IHC staining. Cells that exceeded a given expression threshold are counted. Low threshold values (on the x axis) indicate strong expression, whereas high threshold values indicate weak expression. All values represent mean ± SEM; n = 4 per genotype. *p < 0.05, **p < 0.01, ***p < 0.001 versus WT.

(K) mPER2::LUC bioluminescence traces from SCN explants from *grk2* cKO mice (red) and VGAT-cre::*grk2*$^{fl/+}$ controls (black). x axis indicates days in culture after second media change. Note the higher amplitude and shorter period in *grk2* cKO mice.

(L–N) Histograms showing (L) period length, (M) amplitude, and (N) amplitude dampening of mPER2::LUC bioluminescence rhythms from WT (gray), VGAT-cre::*grk2*$^{fl/+}$ (black), and *grk2* cKO (red) SCN explants following the second media change. n = 6–12 per genotype.

(O) Bioluminescence traces from mPER2::LUC MEFs that were transfected with negative control (NC) or *grk2* siRNA.

(P) Period length of NC or *grk2* siRNA-transfected mPER2::LUC MEFs. n = 4 per condition per experiment. Experiment was performed three times with similar results.

*p < 0.05, **p < 0.01 versus WT and VGAT-cre::*grk2*$^{fl/+}$ (L), versus VGAT-cre::*grk2*$^{fl/+}$ (M), or versus NC siRNA (P). See also Figure S2.

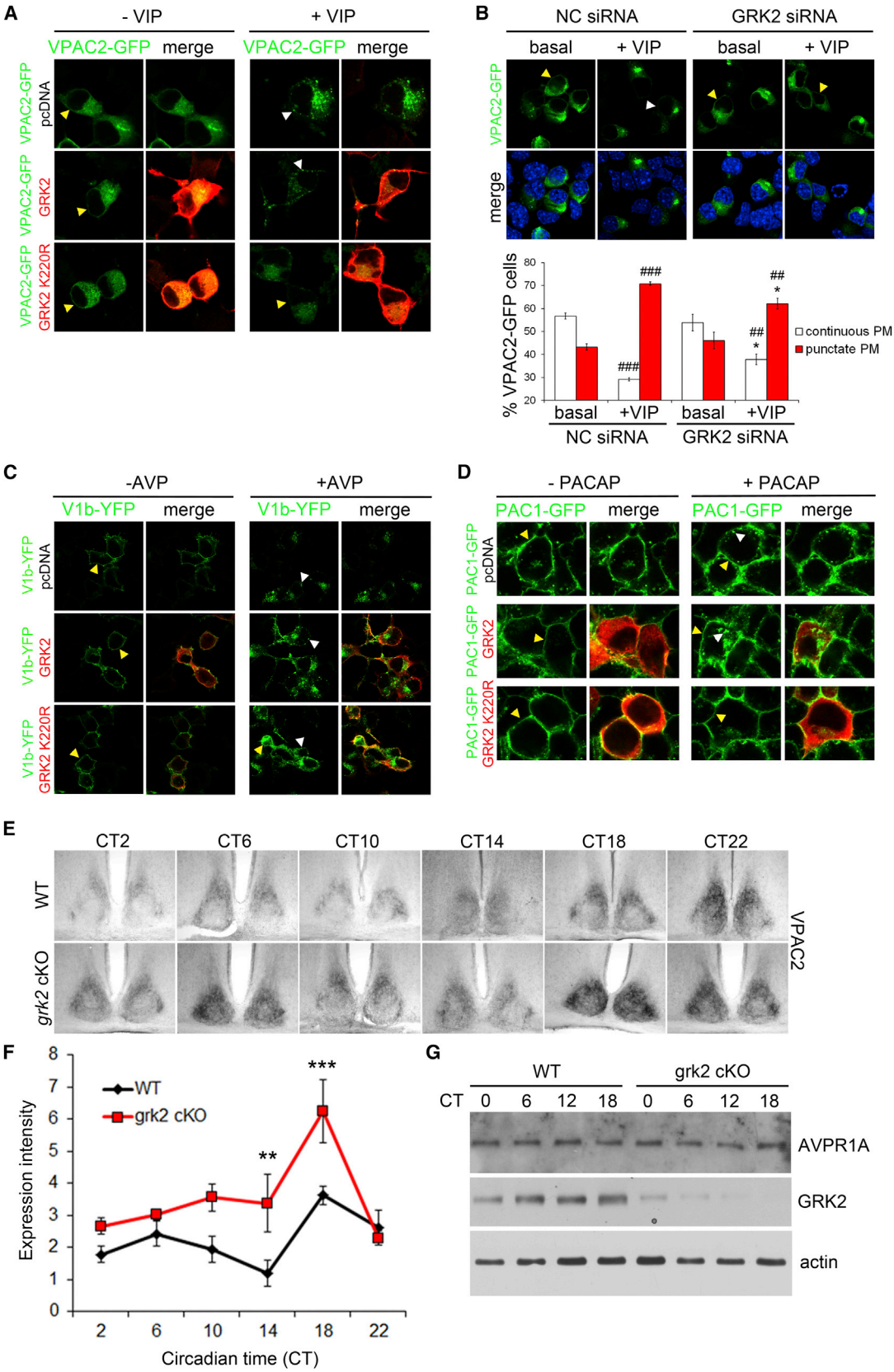

(legend on next page)

the SCN of *grk2* cKO mice throughout the circadian cycle may reflect a compensatory change in the VIP-VPAC2 system in response to increased receptor abundance (Figures S3E and S3F). The effects of GRK2 are not generalized to all GPCRs, since we found no substantial change in the abundance of V1a receptors (the dominant AVP receptor subtype in the SCN) (Figure 3G) or AVP (Figures S3E and S3G) in the mutant SCN.

Collectively, our data suggest that GRK2 regulates ligand-induced internalization of VPAC2 and PAC1 receptors. In the absence of GRK2, total VPAC2 levels are elevated in the SCN along with a compensatory reduction in VIP.

GRK2 Regulates Light-Triggered ERK Activation and *mPeriod1* Gene Transcription

Next, we turned our attention to the effects of *grk2* ablation on PER protein abundance. To explain the changes at the protein level, we focused on *period* gene transcription as a potential mechanism. We started by examining the p44/p42 mitogen-activated protein kinase (MAPK)/ERK pathway, which has been shown to couple light to *period* gene transcriptional activation and clock resetting within the SCN (Butcher et al., 2002; Dziema et al., 2003; Antoun et al., 2012). In wild-type SCN, a brief light pulse (LP: 80 lux, 15 min) in the early (CT 15) and late (CT 22) subjective night, but not mid subjective day (CT 6), induces robust phospho-activation of ERK1/2 (pERK1/2) relative to dark-treated (DD) controls (Figures 4A and 4B). ERK1/2 activation in response to early and late night light exposure was further augmented in the SCN of *grk2* cKO mice (Figures 4A and 4B). These data are consistent with the notion that elevated ERK activation underlies the exaggerated phase delays observed in *grk2* cKO mice. However, a similar enhancement in pERK induction in the late night is not sufficient for promoting phase advances in these animals; additional molecular events specific to the late night may be required in conjunction with ERK activation to mediate phase advances.

We then investigated the effects of GRK2 on *Per1* gene transcription using a bacterial artificial chromosome (BAC) transgenic mouse model that expresses destabilized, nuclear VENUS fluorescent protein under the control of the *mPer1* gene (*mPer1*-VENUS) (Cheng et al., 2009). This strain was bred onto a $grk2^{+/-}$ background. A CT 15 LP not only evoked greater ERK activation in the SCN of $grk2^{+/-}$ mice compared with WT (Figures S4A and S4B) but also resulted in a magnified fold-induction of *mPer1*-VENUS abundance in the core SCN of $grk2^{+/-}$ mice, as a consequence of both lower basal (DD) levels at CT 19 and higher expression following the LP (Figures 4C and 4E). In contrast, *mPer1*-VENUS induction following a CT 22 LP was comparable between WT and $grk2^{+/-}$ mice (Figures S4C and S4D). Importantly, circadian rhythms of *mPer1* transcription were also altered in the SCN of $grk2^{+/-}$ mice, which displayed heightened amplitude of *mPer1*-VENUS oscillations resulting from elevated peak expression at CT 10 and suppressed trough expression at CT 19 (Figures 4D and 4F). The effects of GRK2 on light-induced and circadian transcription of *mPer1* were confirmed using qRT-PCR to compare levels of endogenous *mPer1* transcripts in the SCN of WT and *grk2* cKO mice (Figure S4E). In contrast, we found no effect of *grk2* ablation on *mPer2* at the transcriptional level (Figure S4F).

The modulatory effects of GRK2 on *mPer1* transcription may rely on key signaling systems. In PAC1-GFP-expressing HEK293 cells, *mPer1* promoter-driven luciferase (luc) reporter activity was robustly induced by PACAP stimulation (Figure 4G). Overexpression of GRK2 abolished PACAP-triggered induction of *mPer1*-luc (Figure 4G). Conversely, *grk2* siRNA-mediated silencing not only enhanced PACAP-induced *mPer1*-luc activity but also elevated basal activity (Figure 4H). U0126, a MEK1/2 inhibitor that blocks ERK1/2 activation, abrogated the effects of *grk2* silencing on basal *mPer1*-luc and suppressed PACAP-induced *mPer1*-luc activation to the same extent in both *grk2* siRNA- and NC siRNA-transfected cultures (Figure 4H). H89, a selective inhibitor of cAMP-dependent protein kinase (PKA), which can feed into the ERK1/2 pathway, abolished the increase in both basal and PACAP-induced *mPer1*-luc activity in *grk2*-silenced cultures without having a marked effect on NC cultures (Figure 4H).

Our data suggest that GRK2 negatively modulates *mPer1* transcription through an ERK1/2- and PKA-dependent mechanism, and this transcriptional effect contributes to the higher-amplitude PER1 protein rhythms observed in the SCN of *grk2* cKO mice. On the other hand, GRK2 does not influence *mPer2* transcription per se, but it may regulate PER2 at the post-transcriptional (or post-translational) level to impact its protein expression.

GRK2 Regulates the Nuclear Localization of PER Proteins

Most clock proteins are under post-translational regulation, which dictates their stability and nuclear trafficking (Ko et al.,

Figure 3. GRK2 Regulates GPCR Internalization In Vitro and VPAC2 Abundance in the SCN In Vivo

(A–D) Representative micrographs illustrating the effects of overexpressing or silencing GRK2 on ligand-induced GPCR internalization. (A–C) Neuro2A cells were transfected with constructs encoding (A and B) GFP-tagged VPAC2 and (C) YFP-tagged V1b receptors along with (A and C) pcDNA empty vector, GRK2, or GRK2 K220R, or (B) NC or *grk2* siRNA. Cells were either stimulated (+) or not stimulated (-, basal) with (A and B) VIP or (C) AVP, and harvested 20 min later to assess receptor internalization by indirect IF using a GFP/YFP-specific antibody. Receptors (green); GRK2 (red); DAPI (blue). Internalized receptors (white arrowheads); plasma membrane-localized receptors (yellow arrowheads). For (B), cells were scored for degree of receptor internalization: a continuous line of VPAC2-GFP fluorescence at the plasma membrane (PM) indicates no/little internalization, whereas punctate (or a discontinuous line of) fluorescence at the PM indicates substantial internalization. Values represent mean ± SEM % VPAC2-GFP cells that show continuous or punctate GFP fluorescence at the PM. $^{*}p < 0.05$ versus NC siRNA; $^{\#\#}p < 0.01$, $^{\#\#\#}p < 0.001$ versus basal. (D) Same as (A) and (C), except that the PAC1-GFP HEK293 stable cell line was used. Cells were stimulated with PACAP for 20 min, and localization of receptors (green) was determined by direct GFP fluorescence. Red indicates GRK2.

(E) Representative micrographs of VPAC2-IR in the SCN of WT and *grk2* cKO mice as a function of CT.

(F) VPAC2-IR intensity in the SCN. Values represent mean ± SEM grayscale intensity. n = 4 mice per genotype per CT. $^{**}p < 0.01$, $^{***}p < 0.001$ versus WT.

(G) WB analysis of AVP V1a receptor (AVPR1A) expression in the SCN of WT and *grk2* cKO mice as a function of CT. Actin was used as the loading control. Slight differences in GRK2 levels in *grk2* cKO SCN samples may be due to incomplete Cre-mediated excision in individual animals.

See also Figure S3.

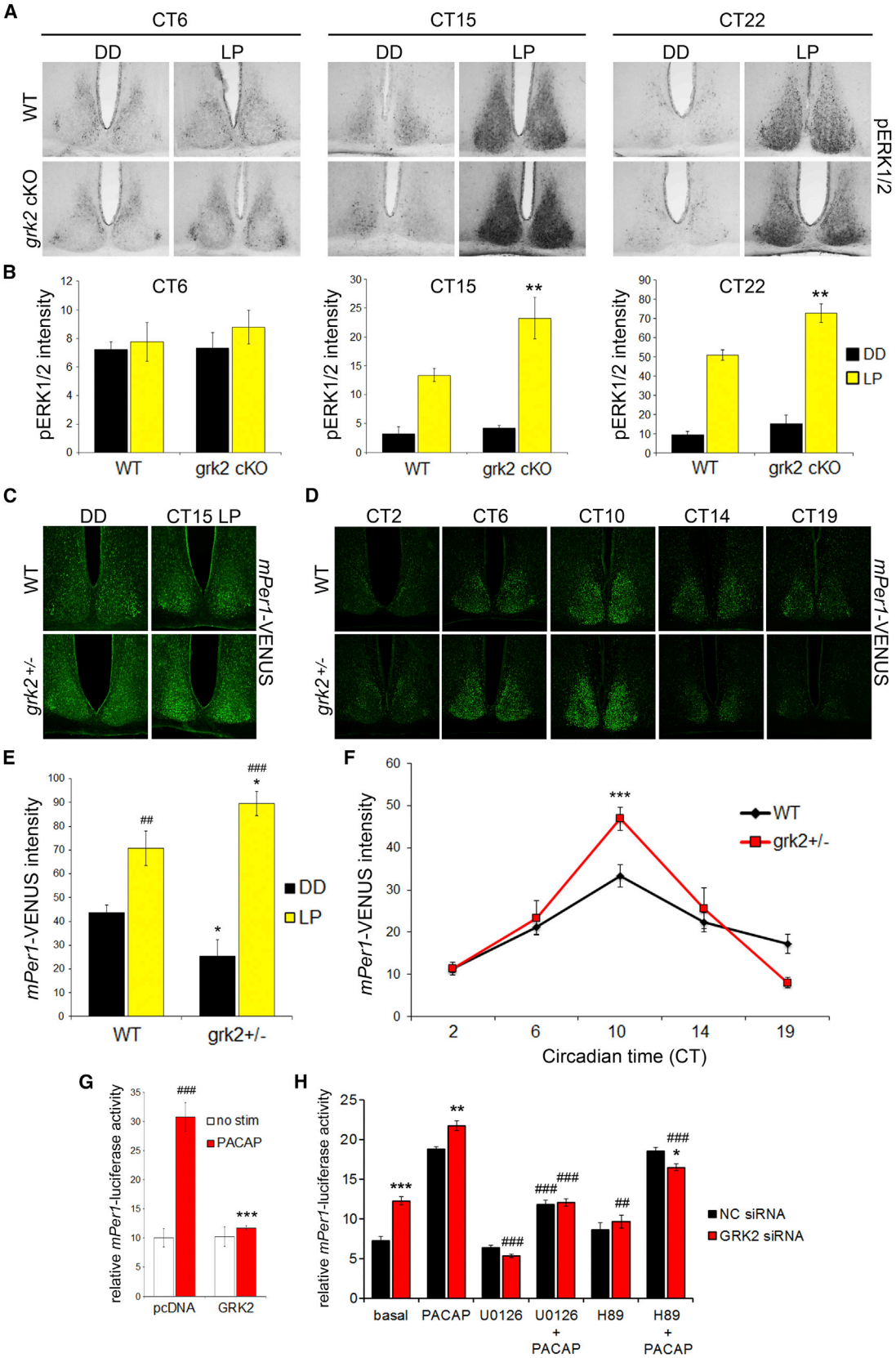

(legend on next page)

2010; Chiu et al., 2008). The shortened PER2::LUC rhythms in *grk2* cKO SCN suggested to us that nuclear trafficking of PER proteins may be facilitated in the absence of GRK2. In line with this hypothesis, the nuclear localization of V5-tagged PER1 (Figures 5A and 5E) and PER2 (Figures 5B and 5F) in Neuro2A cells was significantly suppressed by overexpression of GRK2. Expression intensity of V5-PER1 (Figure 5I) and V5-PER2 (Figure 5J) was suppressed in the nucleus and elevated in the cytoplasm of GRK2-overexpressed cells compared with pcDNA3.1-transfected control cells. These effects of GRK2 overexpression were specific to PER1 and PER2 and were not observed with V5-CRY1 (Figures S5A–S5C), V5-CRY2 (Figures 5C, 5G, and 5K), or myc-BMAL1 (Figures 5D, 5H, and 5L). In the reciprocal experiment, *grk2* siRNA-mediated knockdown resulted in a significant reduction in cytoplasmic localization of V5-PER2 and promoted its redistribution to the nucleus (Figure 5M). *grk2* siRNA did not further promote the nuclear localization of V5-PER1, which was already highly enriched in the nuclei of NC siRNA-transfected Neuro2A cells (Figures S5D and S5E). However, when we examined the nucleocytoplasmic expression of endogenous PER1 in 4-day-old dispersed SCN neuronal cultures, the distribution in GABAergic neurons was shifted toward higher nuclear enrichment of PER1 in *grk2* cKO cultures compared with WT cultures (Figure 5N). Lastly, we quantified the intensities of nuclear and cytoplasmic PER1 and PER2 expression in the intact SCN during the rising phase of their protein rhythms, at CT 12 and CT 15, respectively. The results show that PER1 (Figure 5O) and PER2 (Figure 5P) intensities in the nucleus and cytoplasm were elevated in *grk2* cKO SCN relative to WT SCN. The overall increase in cellular PER in the mutant background may be attributed to enhanced transcription (in the case of *mPer1*) or enhanced protein stability (potentially in the case of PER2). The cumulative evidence suggests that GRK2 suppresses nuclear trafficking of PER1 and PER2, delaying their accumulation in the nucleus.

GRK2 Functionally Converges with Other Protein Kinases to Regulate Nuclear Trafficking of PER Proteins

Nuclear translocation of PER proteins depend on their phosphorylation by specific protein kinases, including casein kinases I delta and epsilon (CK1δ and CK1ε) (Meng et al., 2010) and glycogen synthase kinase 3β (GSK3β) (Iitaka et al., 2005). To address potential functional interplay between GRK2 and other protein kinases in the regulation of PER nuclear trafficking, we determined whether GRK2-dependent suppression of V5-PER1/2 nuclear accumulation was sensitive to pharmacological inhibition of other kinase pathways. Cytoplasmic retention of V5-PER1 through GRK2 overexpression was partially blocked by pre-treatment with the CK1δ/ε inhibitor PF-670462 (Figures 6A–6C). Pharmacological inhibition of GSK3β, MEK1/2, and PKA using LiCl, U0126, and H89, respectively, had no effect on nuclear-cytoplasmic localization of V5-PER1 in either GRK2- or pcDNA3.1-transfected cultures (Figures S6A, S6B, S6D, and S6E). However, U0126 significantly increased V5-PER1 abundance in the cytoplasm of GRK2 transfected cells (Figure S6C), whereas H89 suppressed V5-PER1 abundance in the nucleus of pcDNA3.1 transfected cells (Figure S6F), potentially through mechanisms that impact protein stability.

In terms of PER2 trafficking, PF-670462 effectively eliminated the difference in nuclear-cytoplasmic distribution of V5-PER2 between *grk2* siRNA- and NC siRNA-transfected cultures by decreasing the pool of cells that expressed V5-PER2 exclusively in the cytoplasm (Figures 6D and 6E). H89 had modest effects on the distribution of V5-PER2, whereas U0126 promoted cytoplasmic retention only upon *grk2* knockdown (Figures 6F and 6G). In keeping with a well-documented role of GSK3β in PER2 localization (Iitaka et al., 2005), LiCl triggered robust cytoplasmic retention in both *grk2* siRNA- and NC siRNA-transfected cultures (Figures 6F and 6G).

CK1δ/ε inhibition evoked similar effects on GRK2-dependent V5-PER1 and V5-PER2 subcellular localization in vitro. To examine the in vivo effects of CK1δ/ε blockade, we injected WT and *grk2* cKO mice with PF-670462 6 hr prior to SCN tissue harvest for immunodetection of PER1 and PER2 at CT 14 and CT 18, respectively. Single-cell analysis revealed the expected increase in number of cells expressing high nuclear levels of PER1 and PER2 in the SCN of vehicle-injected *grk2* CKO mice compared with vehicle-treated WT controls (Figures 6H and 6I). This phenotypic difference between WT and *grk2* cKO mice was abolished by PF-670462 pre-treatment, which strongly increased PER1 and PER2 nuclear expression in WT mice but had a more modest effect in *grk2* cKO mice (Figures 6H and 6I). Similar effects of PF-670462 on PER1 localization were observed in $grk2^{+/-}$ mice and WT controls (Figures S6G and S6H). Using the *mPer1*-VENUS transgene on a $grk2^{+/-}$ background, we further showed that the effects of PF-670462 are

Figure 4. Loss of GRK2 Enhances ERK Activation and *Period1* Gene Transcription in the SCN

(A) Representative micrographs of pERK1/2 expression in the SCN of WT and *grk2* cKO mice following a 15 min LP at CT 6, CT 15, or CT 22. Tissues were harvested 30 min after LP onset. Dark controls (DD) were killed at the same time.

(B) pERK1/2 intensity in the shell SCN at CT 6, and in the core SCN at CT 15 and CT 22.

(C and D) Representative micrographs of VENUS-IR in the SCN of WT and $grk2^{+/-}$ mice carrying the *mPer1*-VENUS transgene (C) 4 hr after a 15 min LP administered at CT 15 or (D) as a function of CT. In (C), DD controls were harvested at CT 19.

(E and F) Venus-IR intensity (E) in the core SCN 4 hr after a CT 15 LP or (F) in the whole SCN as a function of CT. All values represent mean ± SEM grayscale/fluorescence intensity. $^{*}p < 0.05$, $^{**}p < 0.01$, $^{***}p < 0.001$ versus WT. $^{\#\#}p < 0.01$, $^{\#\#\#}p < 0.001$ versus DD.

(G) Overexpression of GRK2 inhibits PACAP-induced *mPer1*-luciferase activity in vitro. PAC1-GFP HEK293 cells were transfected with *mPer1* promoter-driven firefly luciferase and constitutively expressed Renilla luciferase (*Rluc*) constructs, along with GRK2 or pcDNA empty vector. Cells were stimulated with PACAP for 6 hr, or were unstimulated, and luciferase activity was measured. Values represent mean ± SEM normalized to *Rluc* activity.

(H) siRNA-mediated *grk2* knockdown enhances *mPer1*-luciferase activity in vitro in a MEK1/2- and PKA-dependent manner. Same as (G), except that cells were transfected with NC or *grk2* siRNA. Following a 30 min pre-treatment with U0126 or H89, cells were stimulated for 6 hr with PACAP in the presence of the kinase inhibitor. Unstimulated cells were treated with DMSO vehicle (basal), U0126 or H89 for 6.5 hr. $^{*}p < 0.05$, $^{**}p < 0.01$, $^{***}p < 0.001$ versus pcDNA or NC siRNA. $^{\#\#}p < 0.01$, $^{\#\#\#}p < 0.001$ versus no stim (G), basal (H), and PACAP alone (H). See also Figure S4.

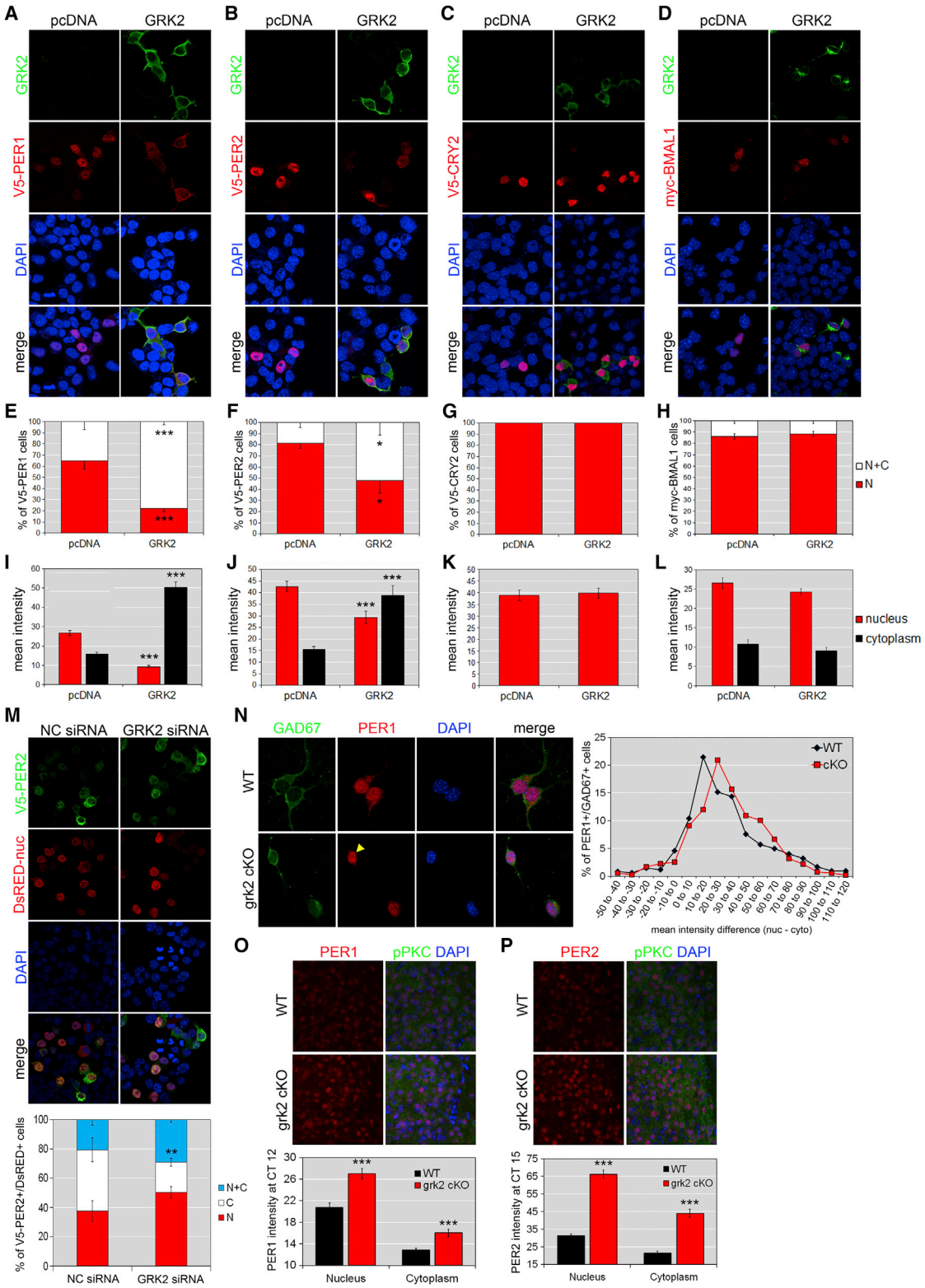

Figure 5. GRK2 Promotes Cytoplasmic Retention and Inhibits Nuclear Accumulation of PER1 and PER2 Proteins

(A–D) Neuro2A cells were transfected with (A) V5-PER1, (B) V5-PER2, (C) V5-CRY2, and (D) myc-BMAL1 (red) along with GRK2 (green) or pcDNA empty vector. (E–H) Percentage of cells expressing (E) V5-PER1, (F) V5-PER2, (G) V5-CRY2, and (H) myc-BMAL1 in the nucleus only (red) or in both the nucleus and cytoplasm (white).

(legend continued on next page)

not dependent on changes in *mPer1* transcription (Figures S6I and S6J). Collectively, our data suggest that GRK2 acts coordinately with CK1δ/ε and other protein kinases to control nuclear-cytoplasmic trafficking of PER1 and PER2.

GRK2 Physically Interacts with PER Proteins and Promotes Phosphorylation of Ser545 on PER2

Our pharmacological results suggest that several protein kinases, including GRK2, CK1δ/ε, GSK3β, and others, coordinately regulate PER1/2 levels in the nucleus and cytoplasm. However, whether GRK2 directly regulates PER1/2 or indirectly regulates them through these other (potential downstream) kinases remains unclear. To address this issue, we probed for protein-protein interactions between GRK2 and V5-PER1/2 using co-immunoprecipitation (coIP). Immunoprecipitation (IP) of FLAG-tagged GRK2 was effective at pulling down V5-PER1 and V5-PER2 (Figure 7A). The reciprocal IP using V5 antibodies also detected a physical association between V5-PER1/2 and GRK2 in total and cytoplasmic protein extracts (Figure 7B). On the other hand, we were unable to coIP GRK2 with FLAG-CK1δ, and vice versa, using YFP-tagged (Figure 7C) and untagged (Figure S7) versions of GRK2.

To test whether GRK2 influences the phosphorylation of PER proteins, we used mass spectrometry to identify residues in V5-tagged murine PER2 that may be differentially phosphorylated upon GRK2 overexpression in Neuro2A cells. Three PER2 phosphosites were identified by MS analysis of the V5 IP fraction: Ser544, Ser545, and Ser624 (Figure 7D). The MS peak intensities for Ser544 and Ser624 fell below the threshold for accurate quantitation. However, Ser545 phosphorylation met the criteria for high confidence quantitation. Compared with pcDNA3.1 controls, overexpression of wild-type GRK2 significantly enhanced Ser545 phosphorylation (Figure 7E). This effect was dependent on the kinase activity of GRK2, and was not observed with GRK2 K220R overexpression (Figure 7E). Furthermore, PF-670462 pre-treatment had no effect on the GRK2-dependent increase in levels of phospho-Ser545 (Figure 7E), indicating that GRK2 mediates Ser545 phosphorylation in a CK1δ/ε-independent manner. Our collective data suggest that GRK2 can physically bind to PER1 and PER2 and promote the phosphorylation of PER2 at Ser545.

DISCUSSION

In this study, we show that GRK2 suppresses *Per1* transcription and nuclear accumulation of PER1/2 in the murine SCN. Consequently, *grk2* cKO mice exhibit higher amplitude of PER1/2 protein rhythms in the SCN, altered behavioral and intrinsic SCN period, and aberrant entrainment to light. Our data further indicate that GRK2 is a binding partner of PER1 and PER2, promoting the phosphorylation of PER2 at Ser545. These findings identify a key role of GRK2 in the transcriptional and post-translational modulation of the SCN circadian clock.

Two entrainment modalities—delays and advances—are differentially affected by the downregulation of GRK2. Light-induced behavioral phase delays are potentiated in *grk2*$^{+/-}$ and *grk2* cKO mice, whereas LD entrainment by advances is decelerated in both *grk2* mutant strains. Acute advances are dependent on *grk2* gene dosage and are attenuated only in *grk2* cKO mice. The phenotypic similarities between grk2$^{+/-}$ and *grk2* cKO mice suggest a threshold effect of GRK2 in some, but not all, aspects of clock function/activity. This is not altogether surprising given that reducing GRK2 levels by 50% (using *grk2*$^{+/-}$ mice) is sufficient to evoke strong phenotypes in various tissues (Vila-Bedmar et al., 2012). Paradoxically, the opposing effects of GRK2 on late-night advances and early-night delays are accompanied by similar elevation of light-induced ERK activation. Previous studies have shown that ERK activation is required for both phase delays and advances (Butcher et al., 2002). However, other signal transduction pathways such as ryanodine receptors and guanylyl cyclase (GC) are phase restricted in their activation, and mediate delays and advances, respectively (Ding et al., 1998; Tischkau et al., 2003). Despite the increase in late-night ERK activation, which should promote, rather than suppress, advances in the *grk2* cKO mice, it is possible that *grk2* ablation disrupts or attenuates GC signaling, overriding the expected effects of ERK. Alternatively, increased ERK activation in the *grk2* cKO SCN in the late night may be aberrantly promoting delay-specific signaling pathways "at the wrong time of day."

Our findings also reveal that GRK2 depletion heightens the amplitude of circadian oscillations in the SCN. PER2::LUC rhythms are higher in *grk2* cKO SCN explants, and peak abundance of PER1 and PER2 was similarly enhanced in the SCN of mutant mice. The amplitude increase is not the consequence of greater interneuronal synchrony within the SCN, as there was no alteration in the dampening of PER2::LUC rhythms ex vivo. Enhanced circadian oscillator amplitude, but not interneuronal coupling, may therefore be a contributing factor to the slower rate of LD re-entrainment observed in *grk2*-deficient mice. The changes in the VIP-VPAC2 system of *grk2* cKO mice are consistent with the lack of a synchrony phenotype: the increase in VPAC2 levels in the SCN, which is predicted to improve synchrony, is offset by reduced abundance of VIP. On the other

(I–L) Mean intensity of (I) V5-PER1, (J) V5-PER2, (K) V5-CRY2, and (L) myc-BMAL1 expression in the nucleus (red) and cytoplasm (black).
(M) Neuro2A cells were transfected with V5-PER2 (green) and nuclear localized DsRED (DsRED-nuc) (red), along with NC or *grk2* siRNA. Graph represents % V5-PER2+/DsRED+ cells that express V5-PER2 in the nucleus only (red), cytoplasm only (white), or nucleus and cytoplasm (blue).
(N) Relative nucleocytoplasmic distribution of endogenous PER1 in cultured primary GABAergic SCN neurons harvested from WT and *grk2* cKO mice. Cells were immunostained for PER1 (red) and GAD67 (green). Yellow arrowhead indicates a cell with predominantly nuclear expression of PER1. Relative intensity distribution was calculated by subtracting the cytoplasmic PER1-IR intensity from the nuclear intensity. Positive values on the x axis indicate nuclear enrichment. The line graph for *grk2* cKO SCN neurons is shifted toward more positive values relative to WT.
(O and P) Levels of (O) nuclear PER1 (red) at CT 12 and (P) nuclear PER2 (red) at CT 15 are enhanced in SCN neurons of *grk2* cKO mice at the upswing of PER1/2 expression. Phospho-PKC (green) was used to delineate the plasma membrane and cytoplasm. Graphs show PER1- or PER2-IR intensity in the nucleus and cytoplasm. All values represent mean ± SEM from three independent experiments.
*$p < 0.05$, **$p < 0.01$, ***$p < 0.001$ versus pcDNA (E–L), NC siRNA (M), or WT (O and P). See also Figure S5.

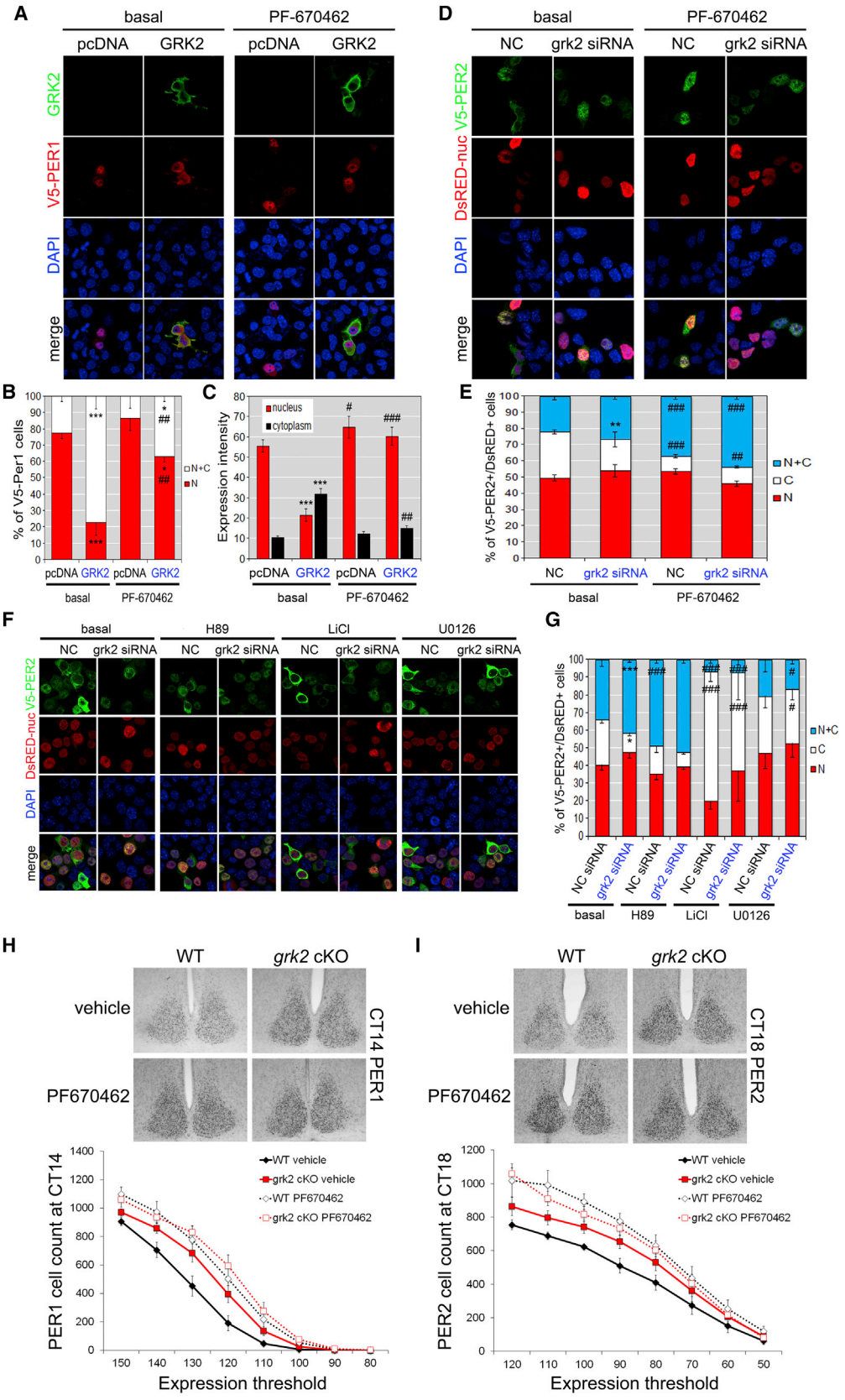

(legend on next page)

hand, the shortening of PER2::LUC rhythms is consistent with the amplitude enhancement, particularly in light of the fact that nuclear PER1/2 levels are greater during the upswing of their rhythms. The divergent effects of *grk2* ablation on behavioral and SCN rhythms suggest that the longer behavioral period of *grk2* cKO mice is not driven by the SCN alone, but rather by interactions between the SCN and extra-SCN oscillators, or between the SCN and its inputs, regardless of whether or not they (i.e., extra-SCN oscillators and inputs) express GRK2. Interestingly, an inverse relationship between behavioral and *Per1-luc* SCN rhythms has also been previously observed, but within the context of non-24-hr light cycles (Aton et al., 2004).

Is it possible that the behavioral phenotypes of *grk2*-deficient mice are the result of dysfunction in retinal inputs rather than the SCN oscillator itself? The fact that GRK2 is also expressed in retinal ganglion cells and regulates melanopsin signaling (Blasic et al., 2012) may, in principle, make it difficult to conclude that the phenotypes are mediated at the level of the SCN. However, our GABAergic neuron-specific cKO model should not ablate *grk2* expression in melanopsin cells, which are intrinsically glutamatergic. Moreover, by isolating the SCN and abolishing afferent inputs, the SCN explant model supports a direct function of GRK2 within the SCN.

What are the underlying mechanisms for the amplitude increase in PER expression in the SCN? Transcriptional regulation of *mPer1* is one causative factor. By reducing *grk2* levels in the SCN, both circadian and light-evoked expression of *mPer1* is enhanced. However, the effects of GRK2 downregulation are specific to *mPer1* and do not extend to *mPer2* expression. *mPer1-luc* reporter assays in cell culture further showed that the facilitatory effects of *grk2* knockdown on basal and PACAP-induced transcription of *mPer1* relied on ERK1/2 and PKA activation. The aggregate evidence suggests that GRK2 suppresses *mPer1* transcription through a CRE-dependent mechanism, which is activated downstream of ERK1/2 and PKA. cAMP-dependent signaling has been shown to sustain the transcriptional feedback loops of the SCN pacemaker, influencing period and amplitude (O'Neill et al., 2008). Although the promoters of *mPer1* and *mPer2* both contain a canonical CRE element within 2 kb of the transcription start site, only the *mPer1* promoter is sensitive to agents that normally trigger CRE-mediated transcription; the *mPer2* promoter is functionally unresponsive despite the ability of CREB to bind to its CRE site (Travnickova-Bendova et al., 2002). On the other hand, given the invariant levels of *mPer2* transcript between mutant and control mice, the increased PER2 abundance in *grk2* cKO SCN may be due to enhancement in translation, protein stability, or both.

Period determination depends on the timing and extent of nuclear accumulation of PER and CRY proteins (Tamanini et al., 2005). The period effects of *grk2* ablation may be explained by a role of GRK2 in the nuclear trafficking of PER1/2 proteins. GRK2 overexpression promotes cytoplasmic retention of mPER1 and mPER2, whereas *grk2* knockdown has the opposite effect on mPER2 localization. The use of ectopic mPER1 and mPER2 sidesteps confounding factors related to endogenous transcription and translation, although it does not eliminate the influence of altered protein stability. Despite the fact that GRK2-dependent PER1/2 cytoplasmic retention was sensitive to CK1δ/ε inhibition in vitro and in vivo, we hesitated to conclude that GRK2 regulates PER1/2 localization specifically through CK1δ/ε as the downstream effector, for two reasons. First, in vitro inhibition of two other kinase pathways, GSK3β and ERK1/2, also had modulatory effects on *grk2* siRNA-dependent PER2 localization. Second, because GRK2 does not physically interact with CK1δ, it becomes difficult to envision a scenario whereby GRK2 can directly regulate the activity of CK1δ on PER proteins. A plausible explanation for our findings is that PER1/2 localization is dictated by the balance of activities among multiple kinase signaling pathways that converge on PER. The effects of certain kinases may be dominant over others (e.g., CK1δ/ε). However, as this study reveals, GRK2 is one kinase pathway that also contributes to the modulation of PER localization.

How might GRK2 affect the behavior of PER1 and PER2? The physical association between GRK2 and PER1/2 not only suggests a direct mode of regulation but also reveals a potential noncanonical function of GRK2. Importantly, GRK2 promotes the phosphorylation of PER2 on Ser545 in a manner dependent on its kinase activity. This residue is phosphorylated by CK1δ in vitro and by endogenous kinases in HEK293 cells (Vanselow et al., 2006). However, GRK2-dependent mPER2 Ser545 phosphorylation was not blocked by PF-670462, suggesting that GRK2 either directly phosphorylates this residue or induces its phosphorylation by a kinase other than CK1δ/ε. Two possible mechanisms may underlie GRK2′s ability to sequester PER1/2 in the cytoplasm. First, GRK2—or a downstream kinase whose activity is induced by GRK2—phosphorylates PER2 at Ser545 to trigger its cytoplasmic retention. Second, GRK2 acts as a scaffold protein to physically retain PER2 (and PER1) in the cytoplasm in a kinase-independent manner. The Ser-545 residue is not conserved in human PER2, suggesting that the scaffold

Figure 6. GRK2 Functionally Converges with CK1δ/ε and Other Prominent Protein Kinase Pathways to Regulate the Nucleocytoplasmic Distribution of PER1 and PER2

(A, D, and F) Neuro2A cells were transfected with (A) V5-PER1 (red) along with GRK2 (green) or pcDNA, or (D and F) V5-PER2 (green) and DsRED-nuc (red) along with NC or *grk2* siRNA. Cells were either mock-treated (basal) or treated for 4 hr with (A and D) PF-670462 or (F) H89, LiCl or U0126.

(B, E, and G) Percentage of (B) V5-PER1+ or (E and G) V5-PER2+/DsRED+ cells that (B) express V5-PER1 in the nucleus only (red) or in both the nucleus and cytoplasm (white), or (E and G) express V5-PER2 in the nucleus only (red), cytoplasm only (white), or both (blue). (C) Mean intensity of V5-PER1 expression in the nucleus (red) and cytoplasm (black). Values represent mean ± SEM from three independent experiments.

(H and I) Nuclear accumulation of PER1 and PER2 in the SCN of *grk2* cKO mice is less sensitive to the effects of PF-670462. Expression of (H) PER1 at CT 14 and (I) PER2 at CT 18 in the SCN of WT and *grk2* cKO mice pretreated with vehicle or PF-670462 6 hr earlier. Histograms show intensity distribution of (H) PER1 at CT 14 and (I) PER2 at CT 18. Cells that exceeded a given expression threshold are counted. Low threshold values indicate strong expression. $^{*}p < 0.05$, $^{**}p < 0.01$, $^{***}p < 0.001$ versus pcDNA. $^{\#}p < 0.05$, $^{\#\#}p < 0.01$, $^{\#\#\#}p < 0.001$ versus basal.

See also Figure S6.

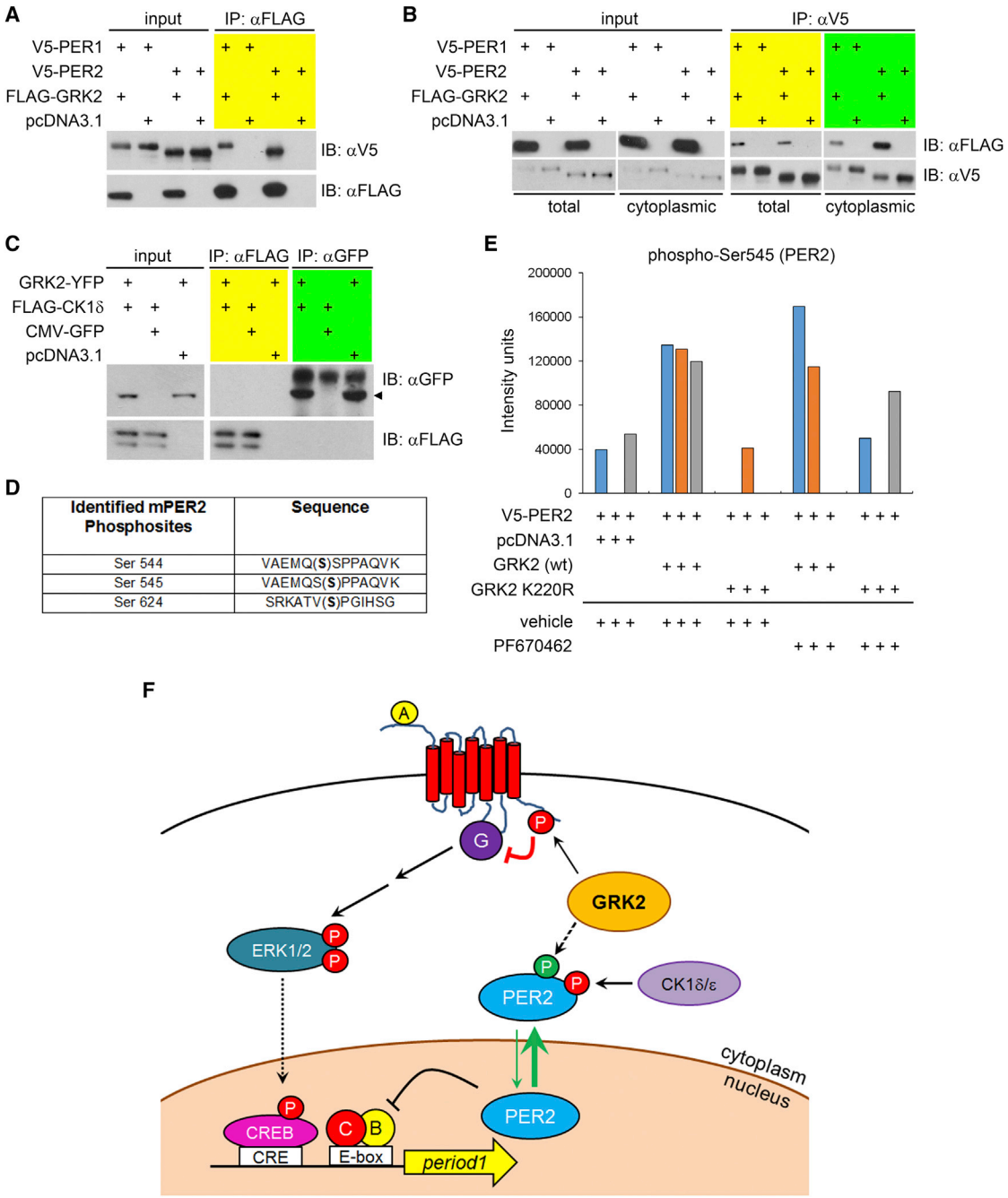

Figure 7. GRK2 Physically Interacts with PER1 and PER2 and Promotes Phosphorylation of PER2 at Ser545

(A and B) Neuro2A cells were transfected with V5-PER1 or V5-PER2 along with FLAG-GRK2 or pcDNA3.1 empty vector. Extracted proteins from total cell lysates or the cytoplasmic fraction were immunoprecipitated (IP) with (A) αFLAG or (B) αV5 antibody-conjugated agarose beads and immunoblotted (IB) with both antibodies.

(C) GRK2 does not physically interact with CK1δ. Neuro2A cells were transfected with GRK2-YFP, FLAG-CK1δ, CMV-GFP (GFP only), or pcDNA3.1 empty vector. IP was performed on total protein lysates using αFLAG or αGFP antibody-conjugated agarose beads and IB with both antibodies.

(D) mPER2 phosphosites identified in our MS experiment. Phosphorylated residue in parentheses.

(E) GRK2 overexpression increases phosphorylation of PER2 at Ser545. Neuro2A cells were transfected with V5-PER2 and either FLAG-GRK2 (wild-type), GRK2 K220R, or pcDNA3.1 empty vector. Cells were treated with PF-670462 or vehicle 4 hr prior to harvesting. IP was performed using αV5 antibody-conjugated beads, and eluates were resolved by SDS-PAGE followed by in-gel digestion prior to MS analysis. Values are given as quantified MS intensity units. Each color represents a biological replicate (n = 3 per condition).

(legend continued on next page)

role of GRK2 may be more pertinent. On the other hand, a greater number of phosphosites have been documented for mPER2 compared with hPER2 (53 versus 15, with 6 overlapping sites; http://www.phosphosite.org), suggesting that there may be species-specific differences in the phosphoregulation of PER2 activity, which in turn might influence interspecies variations in circadian period. The multiple phosphorylation sites on PER is consistent with observations that multiple protein kinases interact synergistically in a temporal order to regulate PER localization through daily changes in phospho-occupancy (Chiu et al., 2008; Ko et al., 2010).

Figure 7F integrates our findings into a hypothetical model of GRK2 function in the SCN. We propose that GRK2 dampens ERK1/2-dependent *mPer1* transcription, through potential modulation of GPCR signaling. In addition, GRK2 acts post-translationally on PER1 and PER2, physically binding to both proteins and promoting the phosphorylation of PER2. We believe that it is through this second, nonclassical pathway that GRK2 modulates the trafficking of PER proteins into the nucleus. Whether or not the physical association with, or phosphorylation of, PER also impacts the stability of PER proteins remains a subject for future investigation.

EXPERIMENTAL PROCEDURES

Animals

Grk2$^{+/-}$ (*Adrbk1*^{tm1Mca}; Jaber et al., 1996), *grk2*$^{fl/fl}$ (*Adrbk1*^{tm1Gwd}; Matkovich et al., 2006), *Vgat*-IRES-Cre knockin (*Slc32a1*$^{tm2(cre)Lowl}$; Vong et al., 2011), mPER2::LUC (Yoo et al., 2004), and *Period1*::VENUS transgenic (Cheng et al., 2009) mouse strains were used in this study. Animal experiments were conducted at the University of Toronto Mississauga animal facility and approved by the local animal care committee in compliance with institutional guidelines and the Canadian Council on Animal Care.

Behavior

Young male mice were housed in running-wheel cages placed within light-tight circadian activity chambers under computer-controlled lighting schedules (Phenome Technologies). For the jetlag paradigm, mice were entrained to a 12-hr light:12-hr dark (LD) cycle before being transferred abruptly to a 7-hr advanced 12:12 LD cycle. For phase-shift experiments, LD-entrained mice were released into constant darkness (DD) for 2 weeks prior to receiving a brief (15 min) light pulse (LP) at circadian time (CT) 15 (30 lux) or CT 22 (40 lux). For constant light (LL) experiments, LD-entrained mice were released into constant dim light (10 lux) for 16 weeks. Behavioral analyses were performed with the ClockLab software (Actimetrics). Period was determined by χ^2 periodogram analysis. Phase shifts were defined as the displacement between two regression lines that were software-fitted through the daily activity onsets 10 days before and 10 days after an LP.

Light Treatment and Tissue Harvest and Processing

Mice were dark-adapted for 2 days prior to further treatment and tissue harvest. For LP experiments, mice received a 15 min LP (80 lux) at the indicated CT and were killed by cervical dislocation at designated times. For in vivo CK1δ/ε inhibition, mice received an intraperitoneal injection of PF-670462 (30 mg/kg) or saline at CT 8 or CT 12 prior to tissue harvest 6 hr later. Coronal SCN tissues were harvested using a vibratome as reported previously (Antoun et al., 2012). For immunolabeling experiments, vibratome sections were fixed (4% paraformaldehyde [PFA] in PBS [pH 7.4]), cryoprotected (30% sucrose in PBS), and cut into 30-μm thin sections using a freezing microtome.

Cell Culture Experiments

Cells were transfected with Lipofectamine 3000 (Life Technologies). 18–24 hr post-transfection, cells were stimulated or treated with pharmacological inhibitors for a prescribed length of time. Cells were either fixed in 4% PFA for subsequent immunostaining, or lysates were prepared for WB or in vitro luciferase assay.

Dispersed SCN Cell Culture

SCN tissues from 6-day-old *Vgat*$^{cre/+}$::*grk2*$^{fl/fl}$ and *grk2*$^{fl/fl}$ pups were dissected, trypsin digested, triturated and plated onto poly-D-lysine-coated glass coverslips. Four days later, cells were fixed with 4% PFA for 20 min and stained for GAD67 and mPERIOD1.

Co-immunoprecipitation

Transfected Neuro2A cells were lysed in lysis buffer supplemented with protease and phosphatase inhibitors. The enrichment of membrane/cytoplasmic cell fractions was performed using published methods (http://www.abcam.com/protocols/subcellular-fractionation-protocol). For the coIP, 0.5–1 mg protein lysate was incubated overnight at 4°C with one of the following: anti-V5 agarose beads (Life Technologies), anti-FLAG M2-agarose beads (Sigma-Aldrich), or 1–2 μg anti-GFP or anti-GRK2 antibody along with TrueBlot anti-rabbit immunoglobulin IP Beads (Rockland Immunochemicals).

Western Blot Analysis

Proteins were separated by SDS-PAGE and immunoblotted for the desired protein as described previously (Antoun et al., 2012).

Luciferase Assay

mPer1-driven firefly luciferase activity in transiently transfected PAC1-HOP1-GFP cells was measured using the Dual Glo Luciferase Assay System (Promega) and normalized to TK-driven Renilla luciferase activity.

Immunohistochemistry, Immunofluorescence, and Immunocytochemistry

Tissue immunohistochemistry and immunofluorescence (IF) were performed as described previously (Antoun et al., 2012). Immunocytochemistry of cultured cells was performed in the same manner as tissue IF.

Imaging and Quantification

Images were acquired using a Zeiss Axio Observer Z1 inverted microscope equipped with a Laser Scanning Microscope (LSM) 700 module (for confocal image acquisition) and an AxioCam MRm Rev.3 monochromatic digital camera (for acquisition of bright-field images, Zeiss), along with the ZEN 2010 software. Images were analyzed using the ImageJ software. The polygon tool was used to outline the region of interest. The "measure" function was used to obtain a "mean gray" value for immunoreactive staining within the specified region. To obtain a normalized "mean gray" value, background "mean gray" values from surrounding non-immunoreactive regions (e.g., lateral hypothalamus) were subtracted from the intensity values. For PER1 and PER2 cell counts across the 24-hr cycle, images were equally assigned a minimum gray-scale threshold of 150 and 160, respectively. The "analyze particle" function was then used to obtain an immunoreactive cell count.

Cultures and Bioluminescence Recordings

Using the Lumicycle-32 instrument (Actimetrics) and published methods (Yamazaki and Takahashi, 2005), we recorded bioluminescence from 300-μm

(F) A proposed model of GRK2-mediated regulation of *mPeriod1* gene transcription and PER nuclear trafficking. Agonist-stimulated GPCRs activate the ERK1/2 pathway in a G-protein-dependent manner, leading to phospho-activation of CREB and CRE-mediated transcription of *mPeriod1*. GRK2 inhibits this pathway through GPCR downregulation. GRK2 also promotes the phosphorylation of PER2, potentially through a direct mechanism, resulting in cytoplasmic retention of PER2. A, receptor agonist; B, BMAL1; C, CLOCK; G, heterotrimeric G protein; P, phosphorylation.
See also Figure S7.

coronal SCN slices from 10- to 15-day-old pups. Period and baseline-subtracted counts were obtained with the Lumicycle Analysis software (version 2.56, Actimetrics) to calculate amplitude and dampening of oscillatory luciferase activity. For bioluminescence recording from immortalized homozygous *Per2*^{Luc} MEFs, cells were transfected with *grk2* siRNA or NC siRNA, and transferred to recording media 4 hr later. Bioluminescence was recorded for 5–7 days.

Mass Spectrometry

Transfected Neuro2A cells (n = 3 biological replicates per condition) were treated with PF-670462 (9 μM) or vehicle for 4 hr prior to harvesting. Cell lysates were incubated with anti-V5 agarose beads (Life Technologies) at 4°C overnight. Eluted proteins were resolved by SDS-PAGE. Gel pieces (~100–250 kDa) were excised for in-gel digestion, and the resulting peptide mixtures were analyzed by an LTQ Velos Pro Orbitrap Elite mass spectrometer (Thermo Fisher Scientific) equipped with a nano-electrospray interface (ekspert nanoLC 400 system) operated in positive ion mode. Separation of peptides was performed on an analytical column (75 μm × 10 cm) packed with reverse phase beads. The instrument method consisted of one full MS scan from 400 to 2000 m/z followed by data-dependent MS/MS scan of the 20 most intense ions, a dynamic exclusion repeat count of 2, and a repeat duration of 90 s. The full mass was scanned in an Orbitrap analyzer with R = 60,000 (defined at m/z 400), and the subsequent MS/MS analyses were performed in LTQ analyzer.

Protein identification was analyzed with MaxQuant (Version 1.3.0.5) using Andromeda as a search engine against the UniProt (release 2013_05) database restricted to Mouse (*Mus musculus*) taxonomy concatenated with a decoy reversed sequences. Spectral counts-based quantitation was carried out using the intensity information in Phospho (STY)Sites file.

Statistical Analyses

One- and two-way analyses of variance (ANOVA) were used to analyze data. Post hoc significance of pairwise comparisons was assessed using Fisher's least significant difference (LSD) tests with α set at 0.05. Statistical analyses were carried out with StatPlus:mac LE (AnalystSoft; http://www.analystsoft.com).

ACCESSION NUMBERS

The mass spectrometry proteomics data have been deposited to the ProteomeXchange Consortium and are available under accession number PXD002290.

SUPPLEMENTAL INFORMATION

Supplemental Information includes Supplemental Experimental Procedures, seven figures, and four tables and can be found with this article online at http://dx.doi.org/10.1016/j.celrep.2015.07.037.

AUTHOR CONTRIBUTIONS

H.-Y.M.C. conceived and designed the study and wrote the paper. C.-K.C. performed and analyzed coIP and MS data. L.M.-V. performed and analyzed SCN bioluminescence and dispersed SCN culture data. H.H.L. and A.P. assisted in cell culture and imaging. B.X. and D.F. assisted in MS experiments and data analysis. N.M., A.H.C., and H.-Y.M.C. performed all other experiments and analyzed the data.

ACKNOWLEDGMENTS

The authors wish to thank the following individuals for contributing valuable reagents: G. Aguilera, M. Caron, N. Cermakian, C. Krasel, S. Laporte, C. Lee, V. May, K. Obrietan, P. Penela, S. Reppert, and D. Weaver. Many thanks to I. Blum for technical advice and all members of the Cheng lab for fruitful discussions. This work was supported by operating grants to H.-Y.M.C. and D.F. from the Canadian Institute of Health Research (CIHR) and the Natural Sciences and Engineering Research Council (NSERC) of Canada. H.-Y.M.C. is a Tier II Canada Research Chair (CRC) in Molecular Genetics of Biological Clocks, and D.F. is a Tier I CRC in Proteomics and Systems Biology. This work is dedicated to the memory of fellow scientist, Heather Dziema-Schutzler.

Received: October 20, 2014
Revised: June 7, 2015
Accepted: July 18, 2015
Published: August 13, 2015

REFERENCES

Akiyama, M., Kouzu, Y., Takahashi, S., Wakamatsu, H., Moriya, T., Maetani, M., Watanabe, S., Tei, H., Sakaki, Y., and Shibata, S. (1999). Inhibition of light- or glutamate-induced mPer1 expression represses the phase shifts into the mouse circadian locomotor and suprachiasmatic firing rhythms. J. Neurosci. *19*, 1115–1121.

Antoun, G., Bouchard-Cannon, P., and Cheng, H.Y. (2012). Regulation of MAPK/ERK signaling and photic entrainment of the suprachiasmatic nucleus circadian clock by Raf kinase inhibitor protein. J. Neurosci. *32*, 4867–4877.

Aton, S.J., Block, G.D., Tei, H., Yamazaki, S., and Herzog, E.D. (2004). Plasticity of circadian behavior and the suprachiasmatic nucleus following exposure to non-24-hour light cycles. J. Biol. Rhythms *19*, 198–207.

Aton, S.J., Colwell, C.S., Harmar, A.J., Waschek, J., and Herzog, E.D. (2005). Vasoactive intestinal polypeptide mediates circadian rhythmicity and synchrony in mammalian clock neurons. Nat. Neurosci. *8*, 476–483.

Blasic, J.R., Jr., Lane Brown, R., and Robinson, P.R. (2012). Light-dependent phosphorylation of the carboxy tail of mouse melanopsin. Cell. Mol. Life Sci. *69*, 1551–1562.

Butcher, G.Q., Doner, J., Dziema, H., Collamore, M., Burgoon, P.W., and Obrietan, K. (2002). The p42/44 mitogen-activated protein kinase pathway couples photic input to circadian clock entrainment. J. Biol. Chem. *277*, 29519–29525.

Cheng, H.Y., Alvarez-Saavedra, M., Dziema, H., Choi, Y.S., Li, A., and Obrietan, K. (2009). Segregation of expression of mPeriod gene homologs in neurons and glia: possible divergent roles of mPeriod1 and mPeriod2 in the brain. Hum. Mol. Genet. *18*, 3110–3124.

Chiu, J.C., Vanselow, J.T., Kramer, A., and Edery, I. (2008). The phospho-occupancy of an atypical SLIMB-binding site on PERIOD that is phosphorylated by DOUBLETIME controls the pace of the clock. Genes Dev. *22*, 1758–1772.

Ding, J.M., Buchanan, G.F., Tischkau, S.A., Chen, D., Kuriashkina, L., Faiman, L.E., Alster, J.M., McPherson, P.S., Campbell, K.P., and Gillette, M.U. (1998). A neuronal ryanodine receptor mediates light-induced phase delays of the circadian clock. Nature *394*, 381–384.

Dziema, H., Oatis, B., Butcher, G.Q., Yates, R., Hoyt, K.R., and Obrietan, K. (2003). The ERK/MAP kinase pathway couples light to immediate-early gene expression in the suprachiasmatic nucleus. Eur. J. Neurosci. *17*, 1617–1627.

Gallego, M., and Virshup, D.M. (2007). Post-translational modifications regulate the ticking of the circadian clock. Nat. Rev. Mol. Cell Biol. *8*, 139–148.

Gurevich, E.V., Tesmer, J.J., Mushegian, A., and Gurevich, V.V. (2012). G protein-coupled receptor kinases: more than just kinases and not only for GPCRs. Pharmacol. Ther. *133*, 40–69.

Iitaka, C., Miyazaki, K., Akaike, T., and Ishida, N. (2005). A role for glycogen synthase kinase-3beta in the mammalian circadian clock. J. Biol. Chem. *280*, 29397–29402.

Jaber, M., Koch, W.J., Rockman, H., Smith, B., Bond, R.A., Sulik, K.K., Ross, J., Jr., Lefkowitz, R.J., Caron, M.G., and Giros, B. (1996). Essential role of beta-adrenergic receptor kinase 1 in cardiac development and function. Proc. Natl. Acad. Sci. USA *93*, 12974–12979.

Ko, H.W., Kim, E.Y., Chiu, J., Vanselow, J.T., Kramer, A., and Edery, I. (2010). A hierarchical phosphorylation cascade that regulates the timing of PERIOD nuclear entry reveals novel roles for proline-directed kinases and GSK-3beta/SGG in circadian clocks. J. Neurosci. *30*, 12664–12675.

Kong, G., Penn, R., and Benovic, J.L. (1994). A beta-adrenergic receptor kinase dominant negative mutant attenuates desensitization of the beta 2-adrenergic receptor. J. Biol. Chem. *269*, 13084–13087.

Matkovich, S.J., Diwan, A., Klanke, J.L., Hammer, D.J., Marreez, Y., Odley, A.M., Brunskill, E.W., Koch, W.J., Schwartz, R.J., and Dorn, G.W., 2nd. (2006). Cardiac-specific ablation of G-protein receptor kinase 2 redefines its roles in heart development and beta-adrenergic signaling. Circ. Res. *99*, 996–1003.

Meng, Q.J., Maywood, E.S., Bechtold, D.A., Lu, W.Q., Li, J., Gibbs, J.E., Dupré, S.M., Chesham, J.E., Rajamohan, F., Knafels, J., et al. (2010). Entrainment of disrupted circadian behavior through inhibition of casein kinase 1 (CK1) enzymes. Proc. Natl. Acad. Sci. USA *107*, 15240–15245.

Moore, R.Y. (2013). The suprachiasmatic nucleus and the circadian timing system. Prog. Mol. Biol. Transl. Sci. *119*, 1–28.

Murthy, K.S., Mahavadi, S., Huang, J., Zhou, H., and Sriwai, W. (2008). Phosphorylation of GRK2 by PKA augments GRK2-mediated phosphorylation, internalization, and desensitization of VPAC2 receptors in smooth muscle. Am. J. Physiol. Cell Physiol. *294*, C477–C487.

O'Neill, J.S., Maywood, E.S., Chesham, J.E., Takahashi, J.S., and Hastings, M.H. (2008). cAMP-dependent signaling as a core component of the mammalian circadian pacemaker. Science *320*, 949–953.

Obrietan, K., Impey, S., and Storm, D.R. (1998). Light and circadian rhythmicity regulate MAP kinase activation in the suprachiasmatic nuclei. Nat. Neurosci. *1*, 693–700.

Penela, P., Murga, C., Ribas, C., Lafarga, V., and Mayor, F., Jr. (2010). The complex G protein-coupled receptor kinase 2 (GRK2) interactome unveils new physiopathological targets. Br. J. Pharmacol. *160*, 821–832.

Reppert, S.M., and Weaver, D.R. (2002). Coordination of circadian timing in mammals. Nature *418*, 935–941.

Tamanini, F., Yagita, K., Okamura, H., and van der Horst, G.T. (2005). Nucleocytoplasmic shuttling of clock proteins. Methods Enzymol. *393*, 418–435.

Tanoue, S., Krishnan, P., Chatterjee, A., and Hardin, P.E. (2008). G protein-coupled receptor kinase 2 is required for rhythmic olfactory responses in Drosophila. Curr. Biol. *18*, 787–794.

Tischkau, S.A., Weber, E.T., Abbott, S.M., Mitchell, J.W., and Gillette, M.U. (2003). Circadian clock-controlled regulation of cGMP-protein kinase G in the nocturnal domain. J. Neurosci. *23*, 7543–7550.

Travnickova-Bendova, Z., Cermakian, N., Reppert, S.M., and Sassone-Corsi, P. (2002). Bimodal regulation of mPeriod promoters by CREB-dependent signaling and CLOCK/BMAL1 activity. Proc. Natl. Acad. Sci. USA *99*, 7728–7733.

Vanselow, K., Vanselow, J.T., Westermark, P.O., Reischl, S., Maier, B., Korte, T., Herrmann, A., Herzel, H., Schlosser, A., and Kramer, A. (2006). Differential effects of PER2 phosphorylation: molecular basis for the human familial advanced sleep phase syndrome (FASPS). Genes Dev. *20*, 2660–2672.

Vila-Bedmar, R., Garcia-Guerra, L., Nieto-Vazquez, I., Mayor, F., Jr., Lorenzo, M., Murga, C., and Fernández-Veledo, S. (2012). GRK2 contribution to the regulation of energy expenditure and brown fat function. FASEB J. *26*, 3503–3514.

Vong, L., Ye, C., Yang, Z., Choi, B., Chua, S., Jr., and Lowell, B.B. (2011). Leptin action on GABAergic neurons prevents obesity and reduces inhibitory tone to POMC neurons. Neuron *71*, 142–154.

Yamazaki, S., and Takahashi, J.S. (2005). Real-time luminescence reporting of circadian gene expression in mammals. Methods Enzymol. *393*, 288–301.

Yoo, S.H., Yamazaki, S., Lowrey, P.L., Shimomura, K., Ko, C.H., Buhr, E.D., Siepka, S.M., Hong, H.K., Oh, W.J., Yoo, O.J., et al. (2004). PERIOD2:LUCIFERASE real-time reporting of circadian dynamics reveals persistent circadian oscillations in mouse peripheral tissues. Proc. Natl. Acad. Sci. USA *101*, 5339–5346.